

A non-iterative reconstruction method for an inverse problem modeled by a Stokes-Brinkmann equations

Mourad Hrizi, Rakia Malek and Maatoug Hassine

Abstract. This article is concerned with the reconstruction of obstacle ω immersed in a fluid flowing in a bounded domain Ω in the two dimensional case. We assume that the fluid motion is governed by the Stokes-Brinkmann equations. We make an internal measurement and then have a least-square approach to locate the obstacle. The idea is to rewrite the reconstruction problem as a topology optimization problem. The existence and the stability of the optimization problem are demonstrated. We use here the concept of the topological gradient in order to determine the obstacle and its rough location. The topological gradient is computed using a straightforward way based on a penalization technique without the truncation method used in the literature. The unknown obstacle is reconstructed using a level-set curve of the topological gradient. Finally, we make some numerical examples exploring the efficiency of the method.

Mathematics Subject Classification (2010). Primary 65M32, 76B75; Secondary 49Q10, 74S30.

Keywords. Inverse problem, Stokes-Brinkmann equations, topological sensitivity analysis.

Contents

1. Introduction	2
2. The problem setting	4
2.1. Notation	4
2.2. The studied problem	4
3. Preliminary results	5
4. Topological sensitivity analysis	8
5. Numerical results	13
5.1. Reconstruction of some obstacles	14
5.2. Influence of the size of the obstacle	15

5.3. Reconstruction results with noisy data	15
6. Concluding remarks	16
Acknowledgements	16
References	16

1. Introduction

This paper is concerned with an inverse problem related to the Stokes-Brinkmann equations. It consists of reconstructing an obstacle immersed in a porous media $\Omega \subset \mathbb{R}^2$ with the help of collecting measurements of the velocity of the fluid motion. Such an inverse problem has several applications, for instance in modeling of liquids or gas through the ground [24, 31] and microfluidics [23].

The number of publications on inverse problems for Stokes-Brinkmann equations are relatively small when compared to Stokes equations, see for instance [1, 12, 11, 7, 19, 2] and reference therein. The works which are related to ours are presented by Lechleiter and Rienmüller [26] and Yan *et al.* [35]. In the first reference, they identified the shape of a penetrable inclusion from boundary measurements using the factorization method. In the work of Yan *et al.*, they solved the considered inverse problem and proposed a method relies on the minimization of a tracking cost functional using the shape gradient method. They derived the shape gradient for the tracking functional based on the continuous adjoint method and the function space parametrization technique.

In our paper, to solve this inverse problem numerically, we propose an alternative method based on the topological sensitivity analysis. The general idea of the proposed method consists in rewriting the inverse problem as a topology optimization problem, where the obstacle is the unknown variable. The topology optimization problem consists in minimizing the so-called least squares functional with the total variation regularization. This cost functional is minimized with respect to a small topological perturbation of the obstacle by using the concept of topological sensitivity. The main advantage of this detection method is that, it provides fast and accurate results for detection.

The topological sensitivity analysis consists of studying the variation of a given cost functional with respect to the presence of a small domain perturbation, such as the insertion of inclusions, cavities, cracks or source-terms. Let us briefly discuss the history of this method. Its main idea was originally introduced by Schumacher [33] in the context of compliance minimization in linear elasticity. In the same context Sokolowski & Zochowski [34], who studied the effect of an extract infinitesimal part of the material in structural mechanics. Then in [27] Masmoudi worked out a topological sensitivity analysis framework based on a generalization of the adjoint method and on the use of a truncation technique. By using this framework the topological sensitivity is obtained for several equations [15, 28, 30, 32]. For other works

on the topological sensitivity concept, we refer to the book by Novotny & Sokolowski [29].

In order to introduce this concept, let us consider a bounded domain $\Omega \subset \mathbb{R}^2$ and a cost function $j(\Omega) = \mathcal{J}(\psi_\Omega)$ to be minimized, where ψ_Ω is the solution to a given partial differential equation defined in Ω . For $\varepsilon > 0$, let $\Omega \setminus \overline{\mathcal{S}_{z,\varepsilon}}$ be the perturbed domain obtained by removing a small topological perturbation $\mathcal{S}_{z,\varepsilon} = z + \varepsilon\mathcal{S}$ from the reference (unperturbed) domain Ω , where $z \in \Omega$ and $\mathcal{S} \subset \mathbb{R}^2$ is a given fixed and bounded domain containing the origin. The topological sensitivity analysis leads to an asymptotic expansion of the function j of the form

$$j(\Omega \setminus \overline{\mathcal{S}_{z,\varepsilon}}) = j(\Omega) + f(\varepsilon)\delta j(z) + o(f(\varepsilon)),$$

where $f(\varepsilon)$ is a positive function depending upon the size ε of the topological perturbation such that $f \rightarrow 0$, when $\varepsilon \rightarrow 0$. The function $z \mapsto \delta j(z)$ is called the “topological gradient” or “topological sensitivity” of j at z . Mathematically, we can express it as

$$\delta j(z) := \lim_{\varepsilon \rightarrow 0} \frac{j(\Omega \setminus \overline{\mathcal{S}_{z,\varepsilon}}) - j(\Omega)}{f(\varepsilon)}.$$

Hence, if we want to minimize the cost function j , the best location to insert a small perturbation in Ω is where δj is most negative. In fact if $\delta j(z) < 0$, we have $j(\Omega \setminus \overline{\mathcal{S}_{z,\varepsilon}}) \leq j(\Omega)$ for small ε . Topological sensitivity analysis for the Stokes equations has been studied in the past by Guillaume and Idris [17], they used the Masmoudi’s approach which is truncation technique. For the quasi-Stokes [18] problems the topological sensitivity has been treated again with the truncation technique. For Navier-Stokes equations, we refer the reader to the work [4], where the topological sensitivity is computed with the help of an alternative to the truncation based on the comparison between the perturbed and the initial problems both formulated in the perforated domain.

In this paper, we have derived a topological asymptotic expansion of the cost functional by using a penalization technique. This approach allowed us to perform the topological asymptotic without using the truncation method presented in the previous works. From the obtained theoretical results, we propose a fast and accurate detection algorithm for recovering the shape and the location of an obstacle. The efficiency and accuracy of the proposed algorithm are illustrated by some numerical examples. Particularly, we test the influence of some parameters in our procedure such as the shape, location and the size of the obstacles.

The rest of this paper is organized as follows. In Section 2, we introduce the notation for function spaces and we present the forward and inverse problem. Section 3 proves the unique existence and the stability of the considered optimization problem. While in Section 4, we derive the asymptotic expansion of the proposed cost functional. In Section 5, some numerical experiments are presented in order to show the effectiveness of the proposed method. Finally, the paper ends with some concluding remarks in Section 6.

2. The problem setting

2.1. Notation

Let us introduce some notation which will be useful in what follows. For an open and bounded domain $\Omega \subset \mathbb{R}^2$, we denote by $L^q(\Omega) := [L^q(\Omega)]^2$ and $H^s(\Omega) := [H^s(\Omega)]^2$ the usual Lebesgue and Sobolev spaces. We define an inner product for matrices by $M : N = \sum_{i,j=1}^2 M_{ij}N_{i,j}$ for $M, N \in \mathbb{R}^{2 \times 2}$; the associated norm is $|M| = \sqrt{M : M}$. The corresponding inner product on $L^2(\Omega)^{2 \times 2}$ is

$$\langle M, N \rangle_{L^2(\Omega)^{2 \times 2}} = \int_{\Omega} M(x) : N(x) \, dx \quad \text{for } M, N \in L^2(\Omega)^{2 \times 2}.$$

In a Banach space \mathcal{Y} , we denote the weak convergence of a sequence $\{\zeta_n\}_n$ to ζ by

$$\zeta_n \rightharpoonup \zeta \quad \text{in } \mathcal{Y} \quad \text{as } n \rightarrow \infty.$$

Finally, for the sake of completeness we briefly introduce the space of functions with bounded total variation. Standard properties of bounded variation functions can be found in [3, 6]. A function u belonging to $L^1(\Omega)$ is said to be of bounded total variation if

$$TV(u) = \int_{\Omega} Du(x) \, dx := \sup \left\{ \int_{\Omega} u \operatorname{div} \varphi \, dx \mid \varphi \in \mathcal{C}_c^1(\Omega, \mathbb{R}^d), \|\varphi\|_{L^\infty(\Omega)} \leq 1 \right\} < \infty.$$

Here $\mathcal{C}_c^1(\Omega, \mathbb{R}^d)$ is the space of continuously differentiable functions with compact support in Ω and $\|\cdot\|_{L^\infty(\Omega)}$ is the essential supremum norm. The space of all functions in $L^1(\Omega)$ with bounded total variation is denoted by

$$BV(\Omega) = \left\{ u \in L^1(\Omega) \mid \int_{\Omega} Du(x) \, dx < \infty \right\}.$$

2.2. The studied problem

Let Ω be a bounded Lipschitz open set of \mathbb{R}^2 containing a Newtonian and incompressible fluid with coefficient of kinematic viscosity $\nu > 0$ and has an inverse permeability $\alpha > 0$. Let ω be a bounded Lipschitz domain included in Ω . The Brinkmann system describing the motion of the fluid in Ω in the presence of the obstacle ω is given by (see, for example [8])

$$\left\{ \begin{array}{ll} -\nu \Delta \psi + \alpha \psi + \nabla p = 0 & \text{in } \Omega \setminus \bar{\omega}, \\ \operatorname{div} \psi = 0 & \text{in } \Omega \setminus \bar{\omega}, \\ \psi = 0 & \text{on } \Gamma, \\ \sigma(\psi, p) \mathbf{n} = g & \text{on } \Sigma, \\ \psi = 0 & \text{on } \partial \omega, \end{array} \right. \quad (2.1)$$

where $g \in H^{-1/2}(\Sigma)$ is a given function, ψ represents the velocity of the fluid and p the pressure and σ represents the stress tensor defined by

$$\sigma(\psi, p) = -p\mathbf{I} + 2\nu e(\psi),$$

with I is the 2×2 identity matrix and $e(\psi)$ is the linear strain tensor defined as

$$e(\psi) = \frac{1}{2} \left(\nabla \psi + {}^t \nabla \psi \right).$$

Here \mathbf{n} denotes the outward normal to the boundary $\partial\Omega = \Sigma \cup \Gamma$ where Σ and Γ have both a nonnegative Lebesgue measure and $\Sigma \cap \Gamma = \emptyset$.

The aim of this work is to reconstruct the obstacle ω . In order to reconstruct the location and the shape of the obstacle, we make a measurement $\psi^d \in H^1(\Omega)$. Thus we consider the following geometric inverse problem:

$$\text{Determine the obstacle } \omega \subset \Omega \text{ from the measurement } \psi^d. \quad (2.2)$$

The data ψ^d for which this inverse problem has a solution ψ are said to be *compatible*.

To solve numerically this geometric inverse problem, we introduce the following optimization problem:

$$\begin{cases} \text{Minimize } \mathcal{K}(\omega, \psi) := J(\omega) = \int_{\Omega \setminus \bar{\omega}} |\psi - \psi^d|^2 dx + \rho \mathcal{P}(\omega, \Omega), \\ \text{subject to } \omega \in \mathcal{U}_{ad} \text{ and } \psi \text{ is the solution to (2.1)} \end{cases} \quad (2.3)$$

where ρ is a regularization parameter and

$$\mathcal{U}_{ad} = \left\{ \omega \subset \Omega : \omega \text{ is a subdomain in } \Omega \text{ such that } \mathcal{P}(\omega, \Omega) < +\infty \right\},$$

with $\mathcal{P}(\omega, \Omega)$ denotes the relative perimeter of ω in Ω is defined by

$$\mathcal{P}(\omega, \Omega) := TV(\chi(\omega)) = \sup \left\{ \int_{\omega} \operatorname{div} \varphi \, dx : \varphi \in \mathcal{C}_c^1(\Omega, \mathbb{R}^2), \|\varphi\|_{L^\infty(\Omega)} \leq 1 \right\}.$$

Here $\chi(\omega)$ is the characteristic function of ω .

Remark 2.1. If $\mathcal{P}(\omega, \Omega) < +\infty$, we say that ω has finite perimeter in Ω . In this case the relative perimeter $\mathcal{P}(\omega, \Omega)$ of ω coincides with the total variation of the distributional gradient of the characteristic function of ω :

$$\mathcal{P}(\omega, \Omega) = |D\chi(\omega)|(\Omega).$$

3. Preliminary results

In this section, we shall establish the unique existence of the solution as well as the stability of the minimization problem (2.3).

Before establishing uniqueness and stability of the minimization problem (2.3), we need the following lemma given in [16, 26].

Lemma 3.1. *The boundary value problem (2.1) admits a unique solution $(\psi(\omega), p(\omega))$ and there exists a constant $c > 0$ such that*

$$\left\| \psi(\omega) \right\|_{H^1(\Omega)} \leq c \left\| g \right\|_{H^{-1/2}(\Sigma)}.$$

Remark 3.2. In the above inequality, the solution $\psi(\omega)$ is extended by zero inside the domain ω , still denoted by $\psi(\omega)$.

The penalization of the cost function (L^2 -norm) by the relative perimeter is relevant for the existence and uniqueness of the optimal solution of (2.3), which will be proved in the following theorem.

Theorem 3.3. *For any $\psi^d \in H^1(\Omega)$, there exists a unique minimizer $\omega^* \in \mathcal{U}_{ad}$ to the minimization problem (2.3).*

Proof. Since $J(\omega)$ is non-negative, we know that $\inf_{\omega \in \mathcal{U}_{ad}} J(\omega)$ is finite. Therefore, there exists a minimizing sequence $\{\omega_n\}_n \subset \mathcal{U}_{ad}$ such that

$$\lim_{n \rightarrow \infty} J(\omega_n) = \inf_{\omega \in \mathcal{U}_{ad}} J(\omega).$$

From the definition of the admissible set \mathcal{U}_{ad} , we have $\mathcal{P}(\omega_n, \Omega) < +\infty$ then $\{\chi(\omega_n)\}_n$ is bounded in $BV(\Omega)$. Thus, $\{\chi(\omega_n)\}_n$ is relatively compact in $L^1(\Omega)$. Therefore, there exists $\omega^* \in \mathcal{U}_{ad}$ and a subsequence of $\{\chi(\omega_n)\}_n$, still denoted by $\{\chi(\omega_n)\}_n$, such that

$$\chi(\omega_n) \rightarrow \chi(\omega^*) \text{ in } L^1(\Omega) \text{ as } n \rightarrow \infty.$$

Now we prove that ω^* is indeed the unique minimizer to the problem (2.3).

Since each ω_n corresponds with a solution $\psi(\omega_n)$ to (2.1) with $\omega = \omega_n$, it follows immediately from Lemma 3.1 that the sequence $\{\psi(\omega_n)\}_n$ is also bounded in $H^1(\Omega)$. This indicates the existence of some $\psi^* \in H^1(\Omega)$ and a subsequence of $\{\psi(\omega_n)\}_n$, again still denoted by $\{\psi(\omega_n)\}_n$, such that

$$\psi(\omega_n) \rightharpoonup \psi^* \text{ in } H^1(\Omega) \text{ as } n \rightarrow \infty. \quad (3.1)$$

We claim $\psi^* = \psi(\omega^*)$. Actually, using Green's formula on (2.1), we have

$$\int_{\Omega \setminus \bar{\omega}} (\nu \nabla \psi : \nabla \vartheta + \alpha \psi \cdot \vartheta) \, dx = \int_{\Sigma} g \cdot \vartheta \, ds, \quad \text{for all } \vartheta \in \mathcal{V}(\omega),$$

where the functional space $\mathcal{V}(\omega)$ is defined by

$$\mathcal{V}(\omega) = \left\{ v \in H^1(\Omega \setminus \bar{\omega}); \operatorname{div} v = 0 \text{ in } \Omega \text{ and } v = 0 \text{ on } \Gamma \cup \partial \omega \right\}.$$

By taking $\omega = \omega_n$ and $\psi = \psi(\omega_n)$ we have

$$\int_{\Omega} \chi(\Omega \setminus \bar{\omega}_n) (\nu \nabla \psi(\omega_n) : \nabla \vartheta + \alpha \psi(\omega_n) \cdot \vartheta) \, dx = \int_{\Sigma} g \cdot \vartheta \, ds, \quad \text{for all } \vartheta \in \mathcal{V}(\omega_n). \quad (3.2)$$

Since (3.1) implies

$$\nabla \psi(\omega_n) \rightharpoonup \nabla \psi^* \text{ in } H^1(\Omega) \text{ as } n \rightarrow \infty,$$

we pass $n \rightarrow \infty$ in (3.2) to obtain

$$\int_{\Omega} \chi(\Omega \setminus \bar{\omega}^*) (\nu \nabla \psi^* : \nabla \vartheta + \alpha \psi^* \cdot \vartheta) \, dx = \int_{\Sigma} g \cdot \vartheta \, ds, \quad \text{for all } \vartheta \in \mathcal{V}(\omega^*).$$

Then it follows from the definition of weak solution and Lemma 3.1 that ψ^* coincides with the unique solution to (2.1) with $\omega = \omega^*$, that is, $\psi^* = \psi(\omega^*)$.

Finally, using $\chi(\omega_n) \rightarrow \chi(\omega^*)$ in $L^1(\Omega)$ and (3.1), we employ the lower semi-continuity of the L^2 -norm and the lower semi-continuity of the perimeter to conclude

$$\begin{aligned} J(\omega^*) &= \int_{\Omega \setminus \overline{\omega^*}} |\psi^* - \psi^d|^2 dx + \rho \mathcal{P}(\omega^*, \Omega) \\ &\leq \liminf_{n \rightarrow \infty} \int_{\Omega \setminus \overline{\omega_n}} |\psi(\omega_n) - \psi^d|^2 dx + \rho \liminf_{n \rightarrow \infty} \mathcal{P}(\omega_n, \Omega) \\ &\leq \liminf_{n \rightarrow \infty} J(\omega_n) = \inf_{\omega \in \mathcal{U}_{ad}} J(\omega). \end{aligned}$$

□

Next, we justify the stability of (2.3), namely, the minimization problem (2.3) that is indeed a stabilization for problem (2.1) with respect to the observation data ψ^d .

Theorem 3.4. *Let $\{\psi_n^d\}_n \subset H^1(\Omega)$ be a sequence such that*

$$\psi_n^d \rightharpoonup \psi^d \text{ in } H^1(\Omega) \text{ as } n \rightarrow \infty, \quad (3.3)$$

and $\{\omega_n\}_n$ be a sequence of minimizer of problems

$$\text{Minimize } J_n(\omega) \text{ with } J_n(\omega) := \int_{\Omega \setminus \overline{\omega}} |\psi - \psi_n^d|^2 dx + \rho \mathcal{P}(\omega, \Omega), \quad n = 1, 2, \dots$$

Then $\{\omega_n\}_n$ converges weakly in $H^1(\Omega)$ to the minimizer of (2.3).

Proof. The unique existence of each ω_n is guaranteed by Theorem 3.3. By definition, we get:

$$J_n(\omega_n) \leq J_n(\omega), \quad \forall \omega \in \mathcal{U}_{ad},$$

which implies the boundedness of $\chi(\omega_n)$ in $BV(\Omega)$. Thus $\chi(\omega_n)$ are relatively compact in $L^1(\Omega)$. Hence, there exists $\omega^* \in \mathcal{U}_{ad}$ and a subsequence of $\{\chi(\omega_n)\}_n$, still denoted by $\{\chi(\omega_n)\}_n$, such that

$$\chi(\omega_n) \rightarrow \chi(\omega^*) \text{ in } L^1(\Omega) \text{ as } n \rightarrow \infty.$$

Now it suffices to show that ω^* is indeed the unique minimizer of (2.3). Actually, repeating the same argument as that in the proof of Theorem 3.3, we can derive

$$\psi(\omega_n) \rightharpoonup \psi(\omega^*) \text{ in } H^1(\Omega) \text{ as } n \rightarrow \infty. \quad (3.4)$$

up to taking a further subsequence. Gathering (3.3) and (3.4), we obtain

$$\psi(\omega_n) - \psi_n^d \rightharpoonup \psi(\omega^*) - \psi^d \text{ in } H^1(\Omega) \text{ as } n \rightarrow \infty.$$

Consequently, for any $\omega \in \mathcal{U}_{ad}$, again we take advantage of the the lower semi-continuity of the L^2 -norm and the lower semi-continuity of the perimeter to

deduce

$$\begin{aligned}
J(\omega^*) &= \int_{\Omega \setminus \overline{\omega^*}} |\psi^* - \psi^d|^2 dx + \rho \mathcal{P}(\omega^*, \Omega) \\
&\leq \lim_{n \rightarrow \infty} \inf \int_{\Omega \setminus \overline{\omega_n}} |\psi(\omega_n) - \psi_n^d|^2 dx + \rho \lim_{n \rightarrow \infty} \inf \mathcal{P}(\omega_n, \Omega) \\
&\leq \lim_{n \rightarrow \infty} \inf \left[\int_{\Omega \setminus \overline{\omega_n}} |\psi(\omega_n) - \psi_n^d|^2 dx + \rho \mathcal{P}(\omega_n, \Omega) \right] \\
&\leq \lim_{n \rightarrow \infty} \left[\int_{\Omega \setminus \overline{\omega}} |\psi(\omega) - \psi_n^d|^2 dx + \rho \mathcal{P}(\omega, \Omega) \right] \\
&= \int_{\Omega \setminus \overline{\omega}} |\psi(\omega) - \psi^d|^2 dx + \rho \mathcal{P}(\omega, \Omega) = J(\omega), \quad \forall \omega \in \mathcal{U}_{ad},
\end{aligned}$$

which verifies that ω^* is the minimizer of (2.3). \square

To solve the minimization problem (2.3), we introduce the topological sensitivity analysis method.

4. Topological sensitivity analysis

In this section, we derive the asymptotic expansion of the cost functional \mathcal{K} with respect to the insertion of a small obstacle $\omega_{z,\varepsilon} \subset\subset \Omega$ that is centered at $z \in \Omega$ and has the form $\omega_{z,\varepsilon} = z + \varepsilon\omega$ where ε is a small parameter and ω is a given bounded domain.

In the presence of the perturbed obstacle $\omega_{z,\varepsilon}$, the velocity ψ_ε and the pressure p_ε solve the following Brinkmann problem:

$$\left\{ \begin{array}{ll} -\nu \Delta \psi_\varepsilon + \alpha \psi_\varepsilon + \nabla p_\varepsilon = 0 & \text{in } \Omega \setminus \overline{\omega_{z,\varepsilon}}, \\ \operatorname{div} \psi_\varepsilon = 0 & \text{in } \Omega \setminus \overline{\omega_{z,\varepsilon}}, \\ \psi_\varepsilon = 0 & \text{on } \Gamma, \\ \sigma(\psi_\varepsilon, p_\varepsilon) \mathbf{n} = g & \text{on } \Sigma, \\ \psi_\varepsilon = 0 & \text{on } \partial \omega_{z,\varepsilon}. \end{array} \right. \quad (4.1)$$

Using the penalization technique used in the finite element method for the implementation of a Dirichlet condition, we can rewrite problem (4.1) as

$$\left\{ \begin{array}{ll} -\nu \Delta \psi_\varepsilon + \alpha \psi_\varepsilon + \delta c_\varepsilon \psi_\varepsilon + \nabla p_\varepsilon = 0 & \text{in } \Omega, \\ \operatorname{div} \psi_\varepsilon = 0 & \text{in } \Omega, \\ \psi_\varepsilon = 0 & \text{on } \Gamma, \\ \sigma(\psi_\varepsilon, p_\varepsilon) \mathbf{n} = g & \text{on } \Sigma, \end{array} \right. \quad (4.2)$$

where δc_ε is a piecewise constant function defined by

$$\delta c_\varepsilon(x) = \begin{cases} k & \text{if } x \in \omega_{z,\varepsilon}, \\ 0 & \text{if } x \in \Omega \setminus \overline{\omega_{z,\varepsilon}}, \end{cases}$$

where k is large enough. The weak form associated with (4.2) reads:

$$\left\{ \begin{array}{l} \text{Find } \psi_\varepsilon \in \mathcal{X}_\Gamma \text{ such that,} \\ \mathcal{A}_\varepsilon(\psi_\varepsilon, v) = l_\varepsilon(v), \quad \forall v \in \mathcal{X}_\Gamma, \end{array} \right. \quad (4.3)$$

where the functional space \mathcal{X}_Γ , the bilinear form \mathcal{A}_ε , and the linear form l_ε are defined by

$$\mathcal{X}_\Gamma = \{v \in H^1(\Omega) \text{ such that } \operatorname{div} v = 0 \text{ and } v = 0 \text{ on } \Gamma\}, \quad (4.4)$$

$$\mathcal{A}_\varepsilon(\psi_\varepsilon, v) = \int_\Omega \nu \nabla \psi_\varepsilon : \nabla v \, dx + \int_\Omega (\alpha + \delta c_\varepsilon) \psi_\varepsilon \cdot v \, dx, \quad (4.5)$$

$$l_\varepsilon(v) = \int_\Sigma g \cdot v \, ds. \quad (4.6)$$

With above statements, we deduce that the cost functional \mathcal{K} is then defined in the perturbed domain as

$$\mathcal{K}(\omega_{z,\varepsilon}, \psi_\varepsilon) = \mathcal{J}(\varepsilon) = \int_\Omega |\psi_\varepsilon - \psi^d|^2 \, dx + \rho \mathcal{P}(\omega_{z,\varepsilon}, \Omega). \quad (4.7)$$

In the particular case $\omega_{z,\varepsilon} = \emptyset$ (i.e, $\varepsilon = 0$), the cost functional \mathcal{K} is defined by L^2 -norm without the regularization term:

$$\mathcal{K}(\emptyset, \psi_0) = \mathcal{J}(0) = \int_\Omega |\psi_0 - \psi^d|^2 \, dx, \quad (4.8)$$

where ψ_0 is the solution to

$$\begin{cases} -\nu \Delta \psi_0 + \alpha \psi_0 + \nabla p_0 = 0 & \text{in } \Omega, \\ \operatorname{div} \psi_0 = 0 & \text{in } \Omega, \\ \psi_0 = 0 & \text{on } \Gamma, \\ \sigma(\psi_0, p_0) \mathbf{n} = g & \text{on } \Sigma. \end{cases} \quad (4.9)$$

The main objective of the following consists in establishing an asymptotic expansion for \mathcal{J} in order to determine the location and shape of ω . Before that, we need the following preliminary lemmas.

Lemma 4.1. *Let ψ_ε and ψ_0 be the solutions to the problems (4.2) and (4.9), respectively. Then, there exists a positive constant c independent of ε such that*

$$\left\| \psi_\varepsilon - \psi_0 \right\|_{H^1(\Omega)} \leq c \varepsilon^{1+\tau},$$

for any $0 < \tau < 1$.

Proof. From (4.2) and (4.9) and using Green's formula, we obtain

$$\begin{aligned} \int_\Omega \nu \nabla (\psi_\varepsilon - \psi_0) : \nabla v \, dx + \int_\Omega (\alpha + \delta c_\varepsilon) (\psi_\varepsilon - \psi_0) \cdot v \, dx \\ + \int_\Omega \delta c_\varepsilon \psi_0 \cdot v \, dx = 0 \quad \forall v \in \mathcal{X}_\Gamma. \end{aligned} \quad (4.10)$$

By taking $v = \psi_\varepsilon - \psi_0$ in (4.10) as a test function, we get

$$\int_\Omega \nu |\nabla (\psi_\varepsilon - \psi_0)|^2 \, dx + \int_\Omega (\alpha + \delta c_\varepsilon) |\psi_\varepsilon - \psi_0|^2 \, dx = - \int_{\omega_{z,\varepsilon}} \psi_0 \cdot (\psi_\varepsilon - \psi_0) \, dx.$$

From the Cauchy-Schwarz inequality and the smoothness of ψ_0 in $\omega_{z,\varepsilon}$, there exists a positive constant c_1 independent of ε such that

$$\begin{aligned} \int_{\Omega} \nu \left| \nabla (\psi_{\varepsilon} - \psi_0) \right|^2 dx + \int_{\Omega} (\alpha + \delta c_{\varepsilon}) \left| \psi_{\varepsilon} - \psi_0 \right|^2 dx &\leq \left\| \psi_0 \right\|_{L^2(\omega_{z,\varepsilon})} \left\| \psi_{\varepsilon} - \psi_0 \right\|_{L^2(\omega_{z,\varepsilon})} \\ &\leq c_1 \varepsilon \left\| \psi_{\varepsilon} - \psi_0 \right\|_{L^2(\omega_{z,\varepsilon})}. \end{aligned}$$

Notice that, Hölder inequality and the Sobolev embedding theorem can be used to derive

$$\left\| \psi_{\varepsilon} - \psi_0 \right\|_{L^2(\omega_{z,\varepsilon})} \leq c_2 \varepsilon^{1/q} \left\| \psi_{\varepsilon} - \psi_0 \right\|_{L^{2p}(\omega_{z,\varepsilon})} \leq c_3 \varepsilon^{\tau} \left\| \psi_{\varepsilon} - \psi_0 \right\|_{H^1(\Omega)},$$

for any $1 < q < \infty$ with $1/p + 1/q = 1$. Let us denote $\tau = 1/q$ which implies $0 < \tau < 1$. Therefore,

$$\int_{\Omega} \nu \left| \nabla (\psi_{\varepsilon} - \psi_0) \right|^2 dx + \int_{\Omega} (\alpha + \delta c_{\varepsilon}) \left| \psi_{\varepsilon} - \psi_0 \right|^2 dx \leq c_4 \varepsilon^{\tau+1} \left\| \psi_{\varepsilon} - \psi_0 \right\|_{H^1(\Omega)}.$$

On the other hand, we have

$$\min\{\nu, \alpha\} \left\| \psi_{\varepsilon} - \psi_0 \right\|_{H^1(\Omega)}^2 \leq \int_{\Omega} \nu \left| \nabla (\psi_{\varepsilon} - \psi_0) \right|^2 dx + \int_{\Omega} (\alpha + \delta c_{\varepsilon}) \left| \psi_{\varepsilon} - \psi_0 \right|^2 dx.$$

Therefore,

$$\left\| \psi_{\varepsilon} - \psi_0 \right\|_{H^1(\Omega)} \leq \frac{c_4 \varepsilon^{\tau+1}}{\min\{\nu, \alpha\}} = c \varepsilon^{\tau+1} \quad \text{with } c = \frac{c_4}{\min\{\nu, \alpha\}}.$$

□

Lemma 4.2. *The cost functional \mathcal{K} is differential with respect to ψ_0 , such that*

$$DK(\emptyset, \psi_0)w = 2 \int_{\Omega} (\psi_0 - \psi^d) \cdot w \, dx \quad \forall w \in H^1(\Omega) \quad (4.11)$$

and we have

$$\mathcal{K}(\omega_{z,\varepsilon}, \psi_{\varepsilon}) - \mathcal{K}(\emptyset, \psi_0) = DK(\emptyset, \psi_0)(\psi_{\varepsilon} - \psi_0) + o(\varepsilon^2). \quad (4.12)$$

Proof. The verification of the differentiability of \mathcal{K} with respect to ψ_0 such that

$$DK(\emptyset, \psi_0)w = 2 \int_{\Omega} (\psi_0 - \psi^d) \cdot w \, dx \quad \forall w \in H^1(\Omega)$$

is trivial.

By subtracting (4.8) from (4.7), we have

$$\begin{aligned} \mathcal{K}(\omega_{z,\varepsilon}, \psi_{\varepsilon}) - \mathcal{K}(\emptyset, \psi_0) &= \int_{\Omega} \left| \psi_{\varepsilon} - \psi^d \right|^2 dx - \int_{\Omega} \left| \psi_0 - \psi^d \right|^2 dx + \rho \mathcal{P}(\omega_{z,\varepsilon}, \Omega) \\ &= \int_{\Omega} \left| (\psi_{\varepsilon} - \psi_0) + (\psi_0 - \psi^d) \right|^2 dx - \int_{\Omega} \left| \psi_0 - \psi^d \right|^2 dx + \rho \mathcal{P}(\omega_{z,\varepsilon}, \Omega) \\ &= 2 \int_{\Omega} (\psi_{\varepsilon} - \psi_0) \cdot (\psi_0 - \psi^d) dx + \int_{\Omega} \left| \psi_{\varepsilon} - \psi_0 \right|^2 dx + \rho \mathcal{P}(\omega_{z,\varepsilon}, \Omega) \\ &= DK(\emptyset, \psi_0)(\psi_{\varepsilon} - \psi_0) + \int_{\Omega} \left| \psi_{\varepsilon} - \psi_0 \right|^2 dx + \rho \mathcal{P}(\omega_{z,\varepsilon}, \Omega), \end{aligned} \quad (4.13)$$

where

$$DK(\emptyset, \psi_0)(\psi_\varepsilon - \psi_0) = 2 \int_{\Omega} (\psi_\varepsilon - \psi_0) \cdot (\psi_0 - \psi^d) dx.$$

Using Lemma 4.1, the second term on the right-hand-side of the equality (4.13) admits the following estimate

$$\int_{\Omega} |\psi_\varepsilon - \psi_0|^2 dx = o(\varepsilon^2).$$

To estimate the last term in the right-hand-side of (4.13), we need to take $\rho = \varepsilon^3$ then,

$$\rho \mathcal{P}(\omega_{z,\varepsilon}, \Omega) = o(\varepsilon^2),$$

since $\mathcal{P}(\omega_{z,\varepsilon}, \Omega) < +\infty$. Therefore;

$$\mathcal{K}(\omega_{z,\varepsilon}, \psi_\varepsilon) - \mathcal{K}(\emptyset, \psi_0) = DK(\emptyset, \psi_0)(\psi_\varepsilon - \psi_0) + o(\varepsilon^2).$$

□

Now, we are ready to state our main result of this section.

Theorem 4.3. *Let $\omega_{z,\varepsilon} = z + \varepsilon\omega$ be a small obstacle in the fluid flow domain Ω and let \mathcal{J} be a cost function of the form*

$$\mathcal{J}(\varepsilon) = \int_{\Omega} |\psi_\varepsilon - \psi^d|^2 dx + \rho \mathcal{P}(\omega_{z,\varepsilon}, \Omega).$$

Then the cost function \mathcal{J} has the following asymptotic expansion:

$$\mathcal{J}(\varepsilon) - \mathcal{J}(0) = k|\omega|\varepsilon^2 \mathcal{G}(z) + o(\varepsilon^2),$$

where $|\omega|$ is the Lebesgue measure (volume) of ω and \mathcal{G} is the topological gradient defined in Ω by

$$\mathcal{G}(z) = \psi_0(z) \cdot \vartheta_0(z),$$

with ϑ_0 is the solution to the adjoint problem: find $\vartheta_0 \in \mathcal{X}_\Gamma$ such that

$$\mathcal{A}_0(w, \vartheta_0) = -DK(\emptyset, \psi_0)w \quad \forall w \in \mathcal{X}_\Gamma. \quad (4.14)$$

Proof. Let us consider the Lagrangian \mathcal{L}_ε defined by

$$\mathcal{L}_\varepsilon(u, v) = \mathcal{K}(\omega_{z,\varepsilon}, u) + \mathcal{A}_\varepsilon(u, v) - l_\varepsilon(v) \quad \forall u, v \in \mathcal{X}_\Gamma.$$

By setting $u = \psi_\varepsilon$ in the above equality and using that ψ_ε is the weak solution to (4.3), we obtain

$$\mathcal{L}_\varepsilon(\psi_\varepsilon, v) = \mathcal{K}(\omega_{z,\varepsilon}, \psi_\varepsilon) \quad \forall v \in \mathcal{X}_\Gamma.$$

Hence,

$$\begin{aligned} \mathcal{J}(\varepsilon) - \mathcal{J}(0) &= \mathcal{L}_\varepsilon(\psi_\varepsilon, v) - \mathcal{L}_0(\psi_0, v) \\ &= \mathcal{K}(\omega_{z,\varepsilon}, \psi_\varepsilon) - \mathcal{K}(\emptyset, \psi_0) + \mathcal{A}_\varepsilon(\psi_\varepsilon, v) - \mathcal{A}_0(\psi_0, v) + l_0(v) - l_\varepsilon(v). \end{aligned} \quad (4.15)$$

The linear form l is independent of ε , then

$$l_0(v) - l_\varepsilon(v) = 0, \quad \forall v \in \mathcal{X}_\Gamma. \quad (4.16)$$

For all $v \in \mathcal{X}_\Gamma$, the variation of the bilinear form is given by

$$\begin{aligned} & \mathcal{A}_\varepsilon(\psi_\varepsilon, v) - \mathcal{A}_0(\psi_0, v) \\ &= \int_{\Omega} \nu \nabla(\psi_\varepsilon - \psi_0) : \nabla v \, dx + \int_{\Omega} \alpha(\psi_\varepsilon - \psi_0) \cdot v \, dx + \int_{\omega_{z,\varepsilon}} k \psi_\varepsilon \cdot v \, dx \\ &= \mathcal{A}_0(\psi_\varepsilon - \psi_0, v) + \int_{\omega_{z,\varepsilon}} k \psi_\varepsilon \cdot v \, dx. \end{aligned}$$

Choosing $v = \vartheta_0$ in the above equality, where ϑ_0 is solution to (4.14), we obtain

$$\mathcal{A}_\varepsilon(\psi_\varepsilon, \vartheta_0) - \mathcal{A}_0(\psi_0, \vartheta_0) = \mathcal{A}_0(\psi_\varepsilon - \psi_0, \vartheta_0) + \int_{\omega_{z,\varepsilon}} k \psi_\varepsilon \cdot \vartheta_0 \, dx.$$

By taking $w = \psi_\varepsilon - \psi_0$ as a test function in (4.14), we deduce that

$$\mathcal{A}_\varepsilon(\psi_\varepsilon, \vartheta_0) - \mathcal{A}_0(\psi_0, \vartheta_0) = -DK(\emptyset, \psi_0)(\psi_\varepsilon - \psi_0) + \int_{\omega_{z,\varepsilon}} k \psi_\varepsilon \cdot \vartheta_0 \, dx. \quad (4.17)$$

Then, it follows from (4.15), (4.16), (4.17) and (4.12) that

$$\mathcal{J}(\varepsilon) - \mathcal{J}(0) = \int_{\omega_{z,\varepsilon}} k \psi_\varepsilon \cdot \vartheta_0 \, dx + o(\varepsilon^2). \quad (4.18)$$

Now we prove that

$$\int_{\omega_{z,\varepsilon}} k \psi_\varepsilon \cdot \vartheta_0 \, dx = k|\omega|\varepsilon^2 \psi_0(z) \cdot \vartheta_0(z) + o(\varepsilon^2).$$

We have

$$\int_{\omega_{z,\varepsilon}} k \psi_\varepsilon \cdot \vartheta_0 \, dx = k \int_{\omega_{z,\varepsilon}} \psi_0 \cdot \vartheta_0 \, dx + k \int_{\omega_{z,\varepsilon}} (\psi_\varepsilon - \psi_0) \cdot \vartheta_0 \, dx. \quad (4.19)$$

Let us first focus on the first term in the right-hand side of (4.19). Using the change of variable $x = z + \varepsilon y$, we derive

$$\begin{aligned} k \int_{\omega_{z,\varepsilon}} \psi_0 \cdot \vartheta_0 \, dx &= k\varepsilon^2 \int_{\omega} \psi_0(z) \cdot \vartheta_0(z) \, dy \\ &\quad + k\varepsilon^2 \int_{\omega} [\psi_0(z + \varepsilon y) \cdot \vartheta_0(z + \varepsilon y) - \psi_0(z) \cdot \vartheta_0(z)] \, dy. \end{aligned}$$

By the Taylor expansion and using the fact that ψ_0 and ϑ_0 are regular near z , we deduce that

$$k\varepsilon^2 \int_{\omega} [\psi_0(z + \varepsilon y) \cdot \vartheta_0(z + \varepsilon y) - \psi_0(z) \cdot \vartheta_0(z)] \, dy = O(\varepsilon^3).$$

Hence,

$$k \int_{\omega_{z,\varepsilon}} \psi_0 \cdot \vartheta_0 \, dx = k|\omega|\varepsilon^2 \psi_0(z) \cdot \vartheta_0(z) + o(\varepsilon^2).$$

For the other term in the right-hand side of (4.19) using Hölder inequality, we derive

$$\begin{aligned} \left| \int_{\omega_{z,\varepsilon}} (\psi_\varepsilon - \psi_0) \cdot \vartheta_0 \, dx \right| &\leq \left\| \vartheta_0 \right\|_{L^2(\omega_{z,\varepsilon})} \left\| \psi_\varepsilon - \psi_0 \right\|_{L^2(\omega_{z,\varepsilon})} \\ &\leq \left\| \vartheta_0 \right\|_{L^2(\omega_{z,\varepsilon})} \left\| \psi_\varepsilon - \psi_0 \right\|_{H^1(\Omega)}. \end{aligned}$$

We know using elliptic regularity that ϑ_0 is uniformly bounded in $\omega_{z,\varepsilon}$. Thus

$$\left\| \vartheta_0 \right\|_{L^2(\omega_{z,\varepsilon})}^2 = \int_{\omega_{z,\varepsilon}} |\vartheta_0|^2 \, dx \leq c \int_{\omega} \varepsilon^2 = O(\varepsilon^2).$$

Consequently,

$$\left| \int_{\omega_{z,\varepsilon}} (\psi_\varepsilon - \psi_0) \cdot \vartheta_0 \, dx \right| \leq c \varepsilon \left\| \psi_\varepsilon - \psi_0 \right\|_{H^1(\Omega)}.$$

From Lemma 4.1, we deduce that

$$\left| \int_{\omega_{z,\varepsilon}} (\psi_\varepsilon - \psi_0) \cdot \vartheta_0 \, dx \right| \leq c \varepsilon^{2+\tau} = o(\varepsilon^2)$$

and the proof is completed. \square

5. Numerical results

In this section, we present some numerical tests showing the efficiency of the proposed method. The aim is to reconstruct the location and shape of an unknown obstacle ω inserted inside the fluid flow domain Ω from internal data by using a level-set curve of the topological gradient.

From Theorem 4.3, the functional \mathcal{K} has the following topological asymptotic expansion:

$$\mathcal{K}(\omega_{z,\varepsilon}, \psi_\varepsilon) = \mathcal{K}(\emptyset, \psi_0) + \varepsilon^2 k \mathcal{G}(z) + o(\varepsilon^2), \quad (5.1)$$

with the function $z \mapsto \mathcal{G}(z)$ is the topological gradient defined by

$$\mathcal{G}(z) = \psi_0(z) \cdot \vartheta_0(z), \quad (5.2)$$

where ψ_0 is the solution to (4.9) and ϑ_0 is the solution of the adjoint problem

$$\begin{cases} -\nu \Delta \vartheta_0 + \alpha \vartheta_0 + \nabla p_0 &= -2(\psi_0 - \psi^d) & \text{in } \Omega, \\ \operatorname{div} \vartheta_0 &= 0 & \text{in } \Omega, \\ \vartheta_0 &= 0 & \text{on } \Gamma, \\ \sigma(\vartheta_0, p_0) \mathbf{n} &= 0 & \text{on } \Sigma. \end{cases} \quad (5.3)$$

The asymptotic expansion (5.1) motivates the reconstruction technique: if we place obstacles in the zone where the topological gradient \mathcal{G} takes pronounced negative values, the error function is expected to decrease, yielding a prediction of the location, shape, size, and number of the obstacles. We identify then a guess for Ω by considering the set

$$\omega_\gamma = \left\{ x \in \Omega; \mathcal{G}(x) \leq (1 - \gamma) \min_{x \in \Omega} \mathcal{G}(x) \right\},$$

where \mathcal{G} is defined by (5.2) and $0 \leq \gamma \leq 1$ is a constant that can be tuned. Therefore, the unknown obstacle ω is likely to be located at the zone where the topological gradient \mathcal{G} is the most negative. To make the numerical simulations presented here, we use a \mathbb{P}_2 finite elements discretization to solve the direct problem (4.9) and the adjoint problem (5.3). The proposed numerical algorithm is based on the following main steps.

One-shot algorithm.

- Solve the direct problem (4.9) and the adjoint problem (5.3).
- Compute the topological gradient $\mathcal{G} = \psi_0 \cdot \vartheta_0$ in Ω .
- Reconstruct the unknown obstacle ω .

The location of ω is given by the point $z \in \Omega$ where the topological gradient \mathcal{G} is most negative (i.e, $z = \arg \min_{x \in \Omega} \mathcal{G}(x)$). The size of ω is approximated as follows

$$\omega = \left\{ x \in \Omega; \mathcal{G}(x) \leq (1 - \gamma^*) \min_{x \in \Omega} \mathcal{G}(x) \right\},$$

where $\gamma^* \in (0, 1)$ such that

$$J(\omega_{\gamma^*}) \leq J(\omega_\gamma) \quad \forall \gamma \in (0, 1),$$

with $\omega_{\gamma^*} = \left\{ x \in \Omega; \mathcal{G}(x) \leq (1 - \gamma^*) \min_{x \in \Omega} \mathcal{G}(x) \right\}$.

The above topological gradient algorithm is classical and has been used to solve various problems [10, 25, 20, 5, 1, 13, 21, 9, 14, 22] and so on.

In this paper, we extend this approach for the reconstruction of obstacle.

Remark 5.1. In the particular case when the exact obstacle ω is known, the best value γ^* of the parameter γ can be determined as the minimum of the following error functional,

$$E(\gamma) = \left[\text{meas}(\omega \cup \omega_\gamma) - \text{meas}(\omega \cap \omega_\gamma) \right] / \text{meas}(\omega), \quad \forall \gamma \in (0, 1), \quad (5.4)$$

where $\text{meas}(H)$ is the Lebesgue measure of the set $H \subset \mathbb{R}^2$.

In all numerical tests, we use synthetic data, i.e., the measurement ψ^d is generated by numerically solving the problem (2.1). The square domain $\Omega = (0, 1) \times (0, 1)$ is used as a mould filled with a viscous and incompressible fluid. For the boundary Σ and Γ , see the sketch in Figure 1.

The approximated solutions are computed using a uniform mesh with $h = 1/100$. The numerical procedure is implemented using the free software *FreeFem++*.

Next, we present some reconstruction results showing the efficiency of the proposed one-shot algorithm.

5.1. Reconstruction of some obstacles

In this section, we study the reconstruction of obstacle having circular or elliptical shapes with no noise added to the simulated data.

Example 1: *Reconstruction of a circular-shaped obstacle.* In this example, we test our procedure to detect an obstacle having circular-shaped. More precisely, we want to reconstruct an obstacle ω described by a disc centered

at $z = (0.5, 0.5)$ with radius $r = 0.05$. The obtained reconstruction results are illustrated in Figure 2.

As one can observe in Figure 2, the unknown obstacle (see Figure 2(b) circle black line) is located in the region where the topological gradient \mathcal{G} is the most negative (see Figure 2(a) red zone) and it is approximated by a level-set curve of the topological gradient (see Figure 2(b) red lines). The result is efficient and the reconstruction of circular shape is very close to the actual obstacle. We also observe the most negative values of the topological gradient which are located near the actual boundary $\partial\omega$.

To reconstruct the exact shape of the actual obstacle in Figure 2(b) (circle centered at $(0.5, 0.5)$ with radius $r = 0.05$ (see Figure 2(b) black line)), we minimize the function E and we take γ^* the minimum of E . To compute numerically an approximation of the minimum of the function E , we divide the interval $(0, 1)$ into ℓ equal subintervals (i.e., of size $1/\ell$). We denote by $\gamma_i = i/\ell$, $1 \leq i \leq \ell$ the $(\ell + 1)$ endpoints of these intervals and we take $\gamma^* = \arg \min_{\gamma \in \{\gamma_1, \dots, \gamma_\ell\}} E(\gamma)$. We represent the results in Figure 3 where the exact boundary $\partial\omega$ represented in black and the obtained shape in red (see Figure 3(b)).

Example 2: Reconstruction of ellipse-shaped obstacle. In this example, we reconstruct an obstacle described by an ellipse centered at $(0.5, 0.5)$. We present the reconstruction results in Figure 4 where we see that the boundary of obstacle (see Figure 4(a)) is again detected and located in the zone where the topological gradient is negative (see Figure 4(a) red lines) and it is approximated by the set ω_{γ^*} where $\gamma^* = 0.15$. Through this test, we show that the proposed method is able to reconstruct approximately the shape and location of obstacle described by an ellipse.

In conclusion of these simulations, this approach permits to give us acceptable knowledge of the location and shape of obstacle having circular or elliptical-shaped. The computation of the topological gradient depends on the size of the obstacle. This remark is illustrated by the following experiments.

5.2. Influence of the size of the obstacle

We now want to study how the size of an obstacle modifies the quality of the detection given by our algorithm. In order to do that, we test how is the detection of a single circle while we increase the radius. For this test, we consider the circle centered at $(0.5, 0.5)$ with radius $r \in \{0.03, 0.06, 0.12, 0.18\}$. The obtained detection results are shown in Figure 5.

From these results, we can notice that, when the obstacle is relatively small, the reconstruction is quite efficient (see Figure 5(a)-(b)), but the quality is decreasing when the obstacle becomes “too big” (see Figure 5(b)-(d)).

Next, we investigate the robustness of the method with respect to noisy measurement.

5.3. Reconstruction results with noisy data

Now we are interested in investigating the robustness of the reconstruction method when the measurement ψ^d is corrupted with Gaussian random noise.

More precisely, the measurement ψ^d is replaced by

$$\psi_\rho^d = \psi^d + \delta\psi^d,$$

where $\delta\psi^d$ is a Gaussian random noise with mean zero and standard deviation $\delta\|\psi^d\|_\infty$, where δ is a parameter.

For this test, we reconstruct an ellipse centered at $(0.5, 0.5)$. The obtained results are illustrated in Figure 6. From the reconstruction results in Figure 6, we can notice that if the noise level no more than 20%, that our algorithm is able to detect the location and the shape of obstacle, whereas for a noise level larger than 30% the reconstruction becomes wrong.

6. Concluding remarks

The presented paper concerns the reconstruction of obstacle immersed in a fluid governed by the Stokes-Brinkmann system in a two-dimensional bounded domain Ω from internal data. In particular, a non-iterative reconstruction method for solving the above inverse problem has been proposed. The general idea consists of rewriting the inverse problem as a topology optimization problem, where a least square functional measuring the misfit between the internal data measurements and the solution obtained from the model is expanded (Stokes-Brinkmann system). The existence and the stability of the optimization problem are proved. We have computed the asymptotic expansion of the cost function using the penalization technique without using the truncation method. The efficiency and accuracy of the reconstruction algorithm are illustrated by some numerical results. The presented method is general and can be adapted for various inverse problems.

In this paper, focused on the topological sensitivity analysis and a non-iterative reconstruction method, several mathematical issues of high interest could not be discussed. The identifiability problem for Stokes-Brinkmann problem is still an open one, will be the subject of a forthcoming work.

Reconstructing obstacle from partial interior observation of the velocity is also an interesting problem to tackle, for several causes may lead to such a situation, especially when zones of the fluid flow domain are not accessible to measurements.

Acknowledgements

The authors would like to thank Professors Maria-Luisa Rapún for many helpful suggestions they made and for the careful reading of the manuscript.

References

- [1] A. B. Abda, M. Hassine, M. Jaoua, and M. Masmoudi. Topological sensitivity analysis for the location of small cavities in stokes flow. *SIAM Journal on Control and Optimization*, 48(5):2871–2900, 2009.

- [2] C. J. Alves and A. L. Silvestre. On the determination of point-forces on a stokes system. *Mathematics and computers in Simulation*, 66(4-5):385–397, 2004.
- [3] L. Ambrosio, N. Fusco, and D. Pallara. *Functions of bounded variation and free discontinuity problems*, volume 254. Clarendon Press Oxford, 2000.
- [4] S. Amstutz. The topological asymptotic for the navier-stokes equations. *ESAIM: Control, Optimisation and Calculus of Variations*, 11(3):401–425, 2005.
- [5] S. Amstutz, I. Horchani, and M. Masmoudi. Crack detection by the topological gradient method. *Control and Cybernetics*, 34(1):81–101, 2005.
- [6] H. Attouch, G. Buttazzo, and G. Michaille. Variational analysis in sobolev and bv spaces: applications to pdes and optimization. 2006.
- [7] E. Beretta, C. Cavaterra, J. H. Ortega, and S. Zamorano. Size estimates of an obstacle in a stationary stokes fluid. *Inverse Problems*, 33(2):025008, 2017.
- [8] T. Borrvall and J. Petersson. Topology optimization of fluids in stokes flow. *International journal for numerical methods in fluids*, 41(1):77–107, 2003.
- [9] M. Burger, B. Hackl, and W. Ring. Incorporating topological derivatives into level set methods. *Journal of Computational Physics*, 194(1):344–362, 2004.
- [10] A. Carpio, T. G. Dimiduk, F. Le Louër, and M. L. Rapún. When topological derivatives met regularized gauss-newton iterations in holographic 3d imaging. *Journal of Computational Physics*, 2019.
- [11] F. Caubet, C. Conca, and M. Godoy. On the detection of several obstacles in 2d stokes flow: topological sensitivity and combination with shape derivatives. 2015.
- [12] F. Caubet and M. Dambrine. Localization of small obstacles in stokes flow. *Inverse Problems*, 28(10):105007, 2012.
- [13] J. Ferchichi, M. Hassine, and H. Khenous. Detection of point-forces location using topological algorithm in stokes flows. *Applied Mathematics and Computation*, 219(12):7056–7074, 2013.
- [14] P. Fulmanski, A. Laurain, J.-F. Scheid, and J. Sokółowski. Level set method with topological derivatives in shape optimization. *International Journal of Computer Mathematics*, 85(10):1491–1514, 2008.
- [15] S. Garreau, P. Guillaume, and M. Masmoudi. The topological asymptotic for pde systems: the elasticity case. *SIAM journal on control and optimization*, 39(6):1756–1778, 2001.
- [16] V. Girault and P.-A. Raviart. *Finite element methods for Navier-Stokes equations: theory and algorithms*, volume 5. Springer Science & Business Media, 2012.
- [17] P. Guillaume and K. S. Idris. Topological sensitivity and shape optimization for the stokes equations. *SIAM Journal on Control and Optimization*, 43(1):1–31, 2004.
- [18] M. Hassine and M. Masmoudi. The topological asymptotic expansion for the quasi-stokes problem. *ESAIM: Control, Optimisation and Calculus of Variations*, 10(4):478–504, 2004.
- [19] H. Heck, G. Uhlmann, and J.-N. Wang. Reconstruction of obstacles immersed in an incompressible fluid. *Inverse Problems and Imaging*, 1(1):63–76, 2007.

- [20] M. Hrzi and M. Hassine. One-iteration reconstruction algorithm for geometric inverse source problem. *Journal of Elliptic and Parabolic Equations*, 4(1):177–205, 2018.
- [21] M. Hrzi, M. Hassine, and R. Malek. A new reconstruction method for a parabolic inverse source problem. *Applicable Analysis*, pages 1–33, 2018.
- [22] M. Jleli, B. Samet, and G. Vial. Topological sensitivity analysis for the modified helmholtz equation under an impedance condition on the boundary of a hole. *Journal de Mathématiques Pures et Appliquées*, 103(2):557–574, 2015.
- [23] D. Köster. Numerical simulation of acoustic streaming on surface acoustic wave-driven biochips. *SIAM Journal on Scientific Computing*, 29(6):2352–2380, 2007.
- [24] M. Krotkiewski, I. S. Ligaarden, K.-A. Lie, and D. W. Schmid. On the importance of the stokes-brinkman equations for computing effective permeability in karst reservoirs. *Communications in Computational Physics*, 10(5):1315–1332, 2011.
- [25] F. Le Louër and M.-L. Rapún. Detection of multiple impedance obstacles by non-iterative topological gradient based methods. *Journal of Computational Physics*, 2019.
- [26] A. Lechleiter and T. Rienmüller. Factorization method for the inverse stokes problem. *Inverse Problems and Imaging*, 7:1271–1293, 2013.
- [27] M. Masmoudi. The topological asymptotic, computational methods for control applications, ed. h. kawarada and j. périaux. *International Series, Gakuto*, 2002.
- [28] M. Masmoudi, J. Pommier, and B. Samet. The topological asymptotic expansion for the maxwell equations and some applications. *Inverse Problems*, 21(2):547, 2005.
- [29] A. A. Novotny and J. Sokołowski. *Topological derivatives in shape optimization*. Springer Science & Business Media, 2012.
- [30] J. Pommier and B. Samet. The topological asymptotic for the helmholtz equation with dirichlet condition on the boundary of an arbitrarily shaped hole. *SIAM journal on control and optimization*, 43(3):899–921, 2004.
- [31] P. Popov, Y. Efendiev, and G. Qin. Multiscale modeling and simulations of flows in naturally fractured karst reservoirs. *Communications in computational physics*, 6(1):162, 2009.
- [32] B. Samet, S. Amstutz, and M. Masmoudi. The topological asymptotic for the helmholtz equation. *SIAM Journal on Control and Optimization*, 42(5):1523–1544, 2003.
- [33] A. Schumacher. *Topologieoptimierung von Bauteilstrukturen unter Verwendung von Lochpositionierungskriterien*. PhD thesis, Forschungszentrum für Multidisziplinäre Analysen und Angewandte Strukturoptimierung. Institut für Mechanik und Regelungstechnik, 1996.
- [34] J. Sokolowski and A. Zochowski. On the topological derivative in shape optimization. *SIAM journal on control and optimization*, 37(4):1251–1272, 1999.
- [35] W. Yan, M. Liu, and F. Jing. Shape inverse problem for stokes-brinkmann equations. *Applied Mathematics Letters*, 88:222–229, 2019.

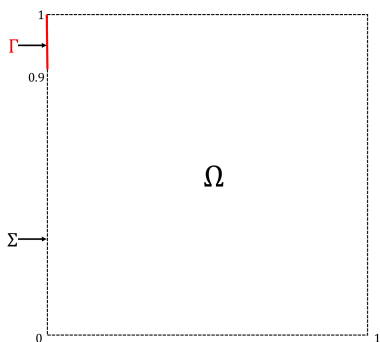
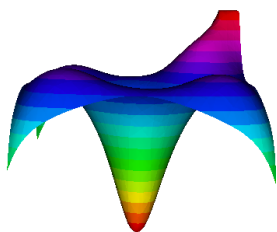
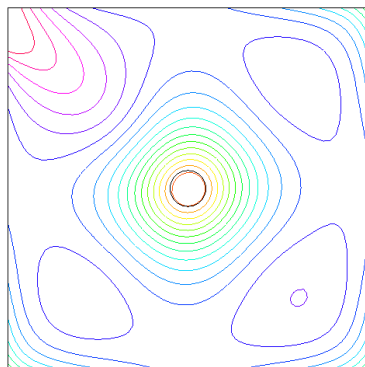


FIGURE 1. Domain Ω with boundary $\partial\Omega = \Sigma \cup \Gamma$



(a) Negative zone (zed zone) of \mathcal{G}



(b) Iso-values of \mathcal{G}

FIGURE 2. Topological gradient \mathcal{G} in the presence of a circle shape

Mourad Hrizi

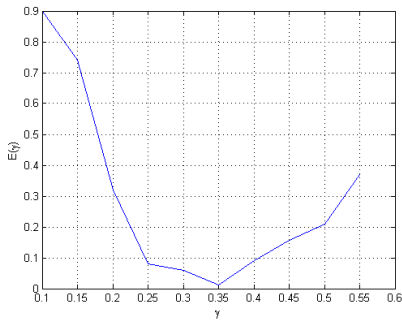
Monastir University, Department of Mathematics, Faculty of Sciences Avenue de l'Environnement 5000, Monastir, Tunisia
e-mail: mourad-hrizi@hotmail.fr

Rakia Malek

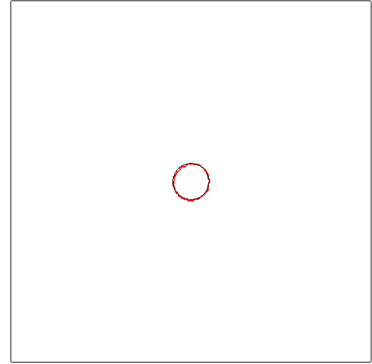
Monastir University, Department of Mathematics, Faculty of Sciences Avenue de l'Environnement 5000, Monastir, Tunisia
e-mail: rakia_malek@hotmail.fr

Maatoug Hassine

Monastir University, Department of Mathematics, Faculty of Sciences Avenue de l'Environnement 5000, Monastir, Tunisia
e-mail: maatoug.hassine@enit.rnu.tn

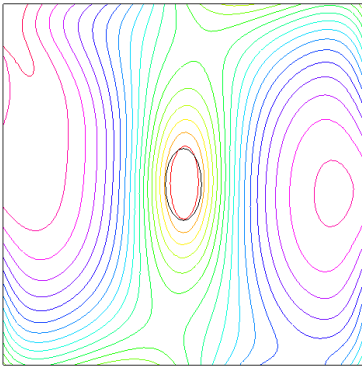


(a) Variation of E with respect to γ

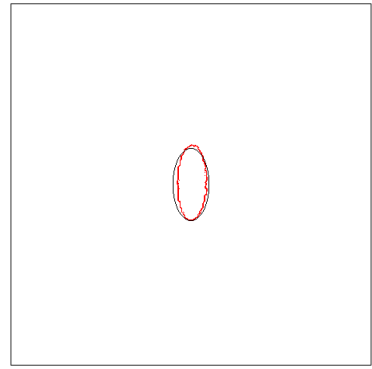


(b) Reconstruction with $\gamma^* = 0.35$

FIGURE 3. Reconstruction of obstacle having a circular-shaped



(a) Iso-values of \mathcal{G}



(b) Reconstruction with $\gamma^* = 0.62$

FIGURE 4. Reconstruction of obstacle having an ellipse-shaped

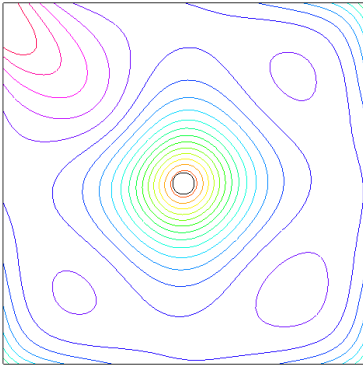
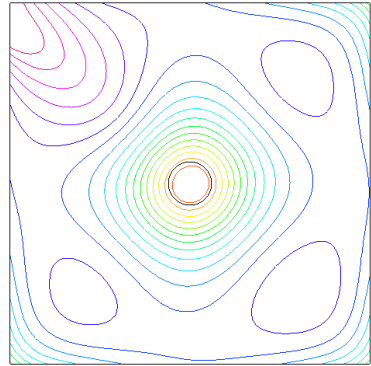
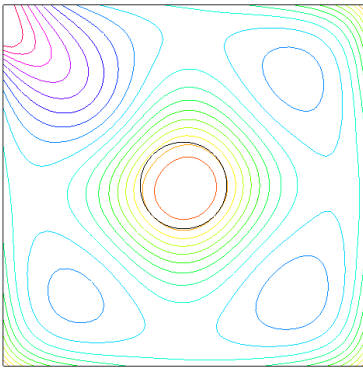
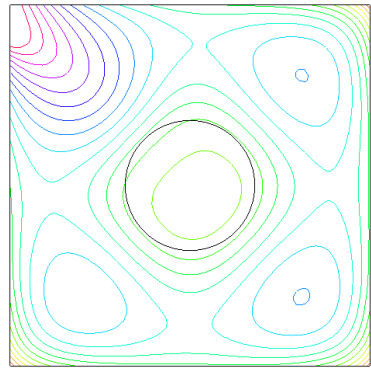
(a) Iso-values of \mathcal{G} with $r = 0.03$ (b) Iso-values of \mathcal{G} with $r = 0.06$ (c) Iso-values of \mathcal{G} with $r = 0.12$ (d) Iso-values of \mathcal{G} with $r = 0.18$

FIGURE 5. Iso-values of the topological gradient when we increase the size of the object

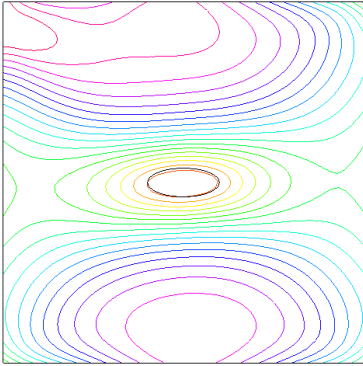
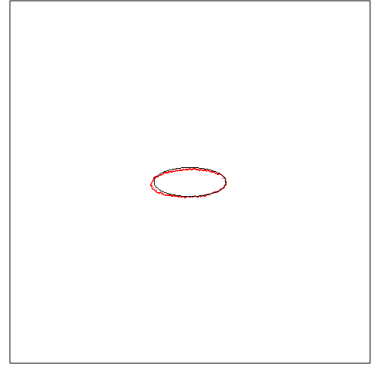
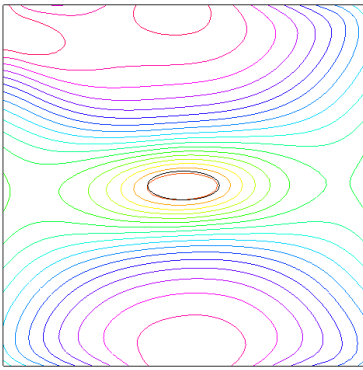
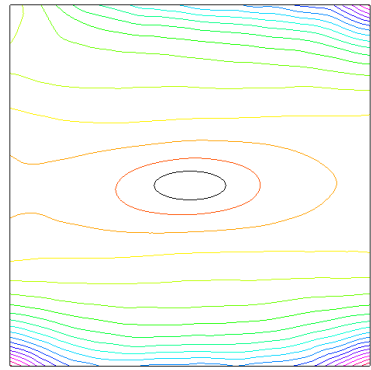
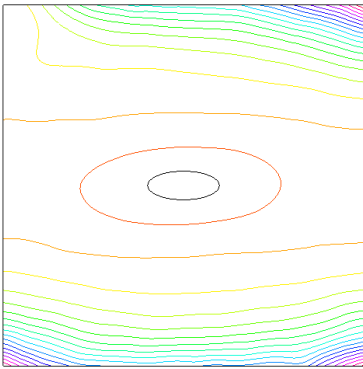
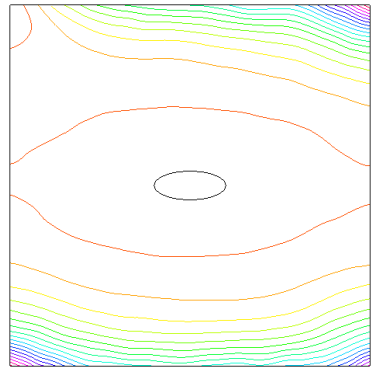
(a) Iso-values of \mathcal{G} with 0% noise(b) Reconstruction with $\gamma^* = 0.63$ (c) Iso-values of \mathcal{G} with 5% noise(d) Iso-values of \mathcal{G} with 10% noise(e) Iso-values of \mathcal{G} with 20% noise(f) Iso-values of \mathcal{G} with 30% noise

FIGURE 6. Reconstruction with noise data